ΤΕΧΝΟΛΟΓΙΚΟ ΠΑΝΕΠΙΣΤΗΜΙΟ ΚΥΠΡΟΥ

ΣΧΟΛΗ ΜΗΧΑΝΙΚΗΣ ΚΑΙ ΤΕΧΝΟΛΟΓΙΑΣ

Μεταπτυχιακή διατριβή

Finite element concrete bridge model analysis and damage scenarios

Αντώνης Λαουτάρης

Λεμεσός [2015]

ΤΕΧΝΟΛΟΓΙΚΟ ΠΑΝΕΠΙΣΤΗΜΙΟ ΚΥΠΡΟΥ

ΣΧΟΛΗ ΜΗΧΑΝΙΚΗΣ ΚΑΙ ΤΕΧΝΟΛΟΓΙΑΣ

ΤΜΗΜΑ ΠΟΛΙΤΙΚΩΝ ΜΗΧΑΝΙΚΩΝ

Finite element concrete bridge model analysis and damage scenarios

του

Αντώνη Λαουτάρη

Λεμεσός [2015]

ΕΝΤΥΠΟ ΕΓΚΡΙΣΗΣ

Μεταπτυχιακή διατριβή

Finite element concrete bridge model analysis and damage scenarios

Παρουσιάστηκε από

Αντώνης Λαουτάρης

Επιβλέπων καθηγητής __Δρ Έλια Ταντελέ_____

Μέλος επιτροπής __Δρ Κρίστης Χρυσοστόμου_____

Μέλος επιτροπής __Δρ Νικόλας Κυριακίδης _____

Τεχνολογικό Πανεπιστήμιο Κύπρου

[Δεκέμβριος, 2015]

Πνευματικά δικαιώματα

Η έγκριση της μεταπτυχιακής διατριβής από το Τμήμα Πολιτικών Μηχανικών του Τεχνολογικού Πανεπιστημίου Κύπρου δεν υποδηλώνει απαραιτήτως και αποδοχή των απόψεων του συγγραφέα εκ μέρους του Τμήματος.

Θα ήθελα να ευχαριστήσω ιδιαίτερα την Άντρη Ορθοδόξου για την σημαντική βοήθεια της στην διεκπαιρείωση αυτής της διατριβής, καθώς και στην οικογένεια μου και να τους αφιερώσω αυτή την διατριβή ως ένδειξη ευχαρίστησης και εκτίμησης προς το πρόσωπο τους.

ΠΕΡΙΛΗΨΗ

Αυτή η μελέτη προτείνει μια ορθολογική μεθοδολογία που χρησιμοποιεί 3D λογισμικό για τη δομική και δυναμική ανάλυση μιας υποθετικής γέφυρας από οπλισμένο σκυρόδεμα και τοποθετείται βάση των γεωγραφικών δεδομένων της Κύπρου. Η συγκεκριμένη μελετη είναι γεωμετρικά συσχετιζόμενη με την Γέφυρα Ζυγού στη Λεμεσό και από την μη γραμμική ανάλυση που προκύπτει απο το πρόγραμμα που χρησιμοποιήθηκε, παρουσιάζονται τα διάφορα πιθανά σενάρια αστοχίας της γέφυρας. Κάθε άνοιγμα υποστηρίζεται σε στηρίγματα μήκους περίπου 15 m. Ως συνέπεια της επαναλαμβανόμενης γεωμετρίας της γέφυρας, οι δοκιμές στη δόνηση λειτουργούσαν σε ένα εύρος χρησιμοποιώντας ένα σύστημα μέριμνας δεδομένων. Ένα 3D μοντέλο πεπερασμένων στοιχείων δημιουργήθηκε και ενημερώνεται για να πάρουμε τιμές που αντιστοιχούν μεταξύ αριθμητικών και πειραματικών τρόπων μεταφοράς ιδιότητων. Στην μελέτη περιλαμβάνονται μετρήσεις πεδίου, αναλυτικές μελέτες επαλήθευσης μοντέλου, καθώς και τα σενάρια αστοχίας. Με τη βοήθεια του CSi Bridge ανάλυσης, σχετικά με περιπτώσεις φόρτισης, δυναμικής ανάλυσης, ο υπολογισμός της διάρκειας ζωής και οι συνδυασμοί φόρτισης που παροθσιάζονται ενδελεχώς σ' αυτή την διατριβή εχουν ως κύριο στόχο την παρουσίαση των διαφόρων σεναρίων αστοχίας της γέφυρας καθώς και το πώς επηρεάζεται από διάφορους άλλους παράγοντες όπως είναι η διάβρωση, η ολική καταστροφή της γέφυρας στην περίπτωση σεισμού, όπως και άλλες περιπτώσεις αστοχίας που αφορούν τοπική καταστροφή και επηρεάζουν την ολική αντοχή της γέφυρας οπου μεταβάλλουν τα κύρια χαρακτηριστικά αυτής.

ΠΙΝΑΚΑΣ ΠΕΡΙΕΧΟΜΕΝΩΝ

ΚΑΤΑΛΟΓΟΣ ΔΙΑΓΡΑΜΜΑΤΩΝ

ΣΥΝΤΟΜΟΓΡΑΦΙΕΣ

Παρουσιάζονται συνοπτικά όλες οι σημαντικές συντομογραφίες που έχουν χρησιμοποιηθεί στο κείμενο της διατριβής π.χ.:

ΤΕΠΑΚ.:	Τεχνολογικό Πανεπιστήμιο Κύπρου
LCC	Live-Cyrcle Cost
ZB	Zygou Bridge

ABSTRACT

This paper proposes a rational methodology using 3D software for the structural and dynamic analysis of a hypothetical reinforced concrete bridge model situated in Cyprus. The case study is geometrically related with the Zygou Bridge in Limassol. The analysis obtained is based on vibration measurement of the bridge, assimilation of its modal signature, restricted element model updating, as well as nonlinear analysis. The selected case study is an nine-span bridge with a continuous deck slap. Each span is simply supported at bearings and has a length of an approximately 15 m. As a consequence of the repetitive geometry of the bridge, vibration tests were operated on one span using a data procuration system. A 3D finite element model was created and updated to obtain reasonable correspond between numerical and experimental modal properties. Field measurements, analytical model verification studies as well as damaged scenarios are situated. With the help of CSi Bridge, load cases, dynamic, time dependence and load combinations analysis is achieved. Furthermore, several damaged scenarios were created in order to investigate the consequences on the object's structure.

INTRODUCTION

Notable progress has been made in the past two decades in creating novel techniques to model the nonlinear behavior of building structures. Many factors have contributed to the rapid development of inelastic models for structures. Some of them are: extensive interest in the behavior of buildings subjected to earthquakes, the unpleased seismic performance of many building components, the short availability of test data regarding building elements subjected to seismic type loading, etc. With the progression of society and economy, more and more attentions have been paid to the safety and serviceability of structures. Evaluation of the actual safety of an existing bridge is very important to a bridge management system. Safety of a bridge is mainly affected by the actual load bearing capacity of its structural elements as well as by the position and load of the moving axis, which in turn control the critical values used in design and analysis. Based on the captured test data, it is also possible to determine the safety level of the actual bridge behavior, as the existing damages on the structural elements. Any measured drop regarding the rigidities of the bridge should be investigated thoroughly to evaluate the fatigue life as well as to decide any renewal or replacement is essential or not. This rapid progression in the field of engineering, lead to the development of software technology programs in order to investigate and prevent essential issues that might appear on the structure.

The increasing significance of condition assessment in civil engineering has created comprehensive research in developing vibration based damage methods. Natural frequencies and mode shapes have found great interest because of the appealing fact that modal parameters are equal of structures. Hence, any structural variation is associated with changes of modal parameters. Moreover, because of the global character of modal parameters, their variations are not circumscribed at the location of damage. This is an essential advantage opening the opportunity to determinate damage with sensors whose location needs not to correspond with the damaged area. The focus on modal parameters was farther substantiate by recent advances in system identification, output only stochastic subspace algorithms, which driven to numerically steady and reliable algorithms to persuade experimentally modal parameters from climate test data see Peeters and De Roeck 2001 for a complete review on this subject.

Reinforced concrete bridges were subjected to continuous deterioration of structural performances and devaluation of structural reliability during their life expectancy due to aggressive environments. In this paper lifetime performance reliability of the bridge under corrosion attacks is presented. It is important to underline that reinforced concrete structures are more delicate strength-wise than steel structures and it has very essential engineering value to analyse the nonlinear structural behavior under the case of over loading factors. Any increase in axle loads specifically coupled with an increased value of AADT (annual average daily traffic) during the service life of a bridge may also result a less safety level than that was assumed before. The current structural state of a bridge may be estimated by using structural identification provided by the model software. Techniques of developing the model using the obtained measurements and experimental identification of the dynamic characteristics of the bridge based on tests carried out have been studied by many researchers.

Although corrosion of concrete in bridge girders is receiving wider attention in recent years due to several cases of failure of prestressed girders in different parts of the world, a realistic mathematical corrosion model of prestressed concrete is not an easy task (Enright, 1998). Deterioration of concrete bridge is dependent on both the behavior of the environment as well as the properties of the prestressed concrete. Environmental factors can be harmful to prestressed concrete which include the presence of moisture, chloride ions, carbon dioxide and cycles of temperatures. Despite the fact that various strength degradation mechanisms are available for concrete structures, strength loss due to corrosion of steel reinforcement is frequently reported mechanism for concrete bridges and corrosion appears after a period known as the corrosion initiation time. For bridges, corrosion initation is normally caused due to chloride ion ingress. Once corrosion has been initiated, the cross-sectional area of reinforcement decreases with time at a rate that is dependent on the number of prestressed steel actively corroding, and the corrosion rate and diameter of the individual steel (Mori et al, 1993)

The theoretical concept regarding concrete design is the transfer that occurs from the compression force from steel strands to surrounding concrete to accomplish a crack free member under service forces. The properties of concrete and the interface of strand cause this

transfer of stress to happen within a short distance from the end of the girder, with big stress conditions. This causes an overstressed girder end region may reveal visible cracks in uncommon patterns. These cracks might affect the durability of the bridge, in the case that they are not enclosed in the end diaphragms or revealed to the environment. In the case of salt water seeped through the cracks and reaches the strands, corrosion and loss of connection between strands and concrete might lead to loss of structural capacity.

1 Description of the bridge

The bridge model was design according to the measurements and the geometry of the Zygou Bridge. The Zygou Bridge, located above Kourri River, is a multi-span concrete bridge that was opened to traffic in 1980. The bridge spans between the city of Limassol and Platres located in the southwestern part of Cyprus. The bridge over water has a double traffic lane, and it is composed of 8 columns with fixed connections each having 9.5m open deck, totaling 126.496m in length. This bridge is currently under reconstruction by Iacovou Brothers Constructions Ltd due to intense erosion and deterioration of building materials. The redevelopment operation will be completed in about 60 weeks. It is a technically complex project, since it includes the demolition of the existing deck, rebuild with an increased width, as well as enhance the carrying capacity of the piers and abutments and creating a bypass road. A general view of the bridge is given in Figure 1. According to the original constructional drawings of the bridge each span is seated on reinforced concrete piers having H hollow cross section with varying heights between 20.2m and 12.6m and abutments. The piers are supported on piled foundations where centre-to-centre distance of piers varies between 12m and 22m. The top surfaces of the piles are connected by a reinforced concrete cap.

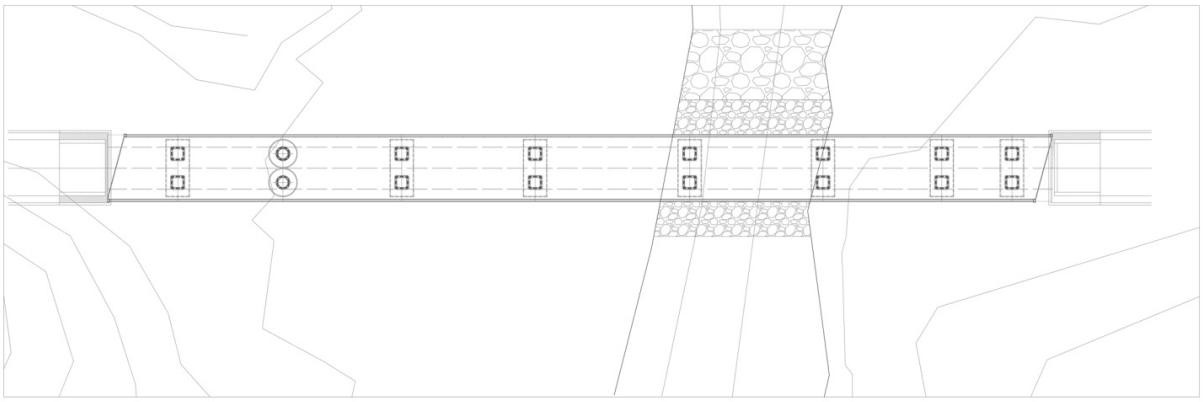

Figure 1: Bridge Plan

The prototype bridge consists of 8 concrete columns, each having an average 15m span length, giving a total bridge length of 126.496m. To understand the actual behavior of the bridge, static and dynamic tests on the bridge spans were performed. A three-dimensional finite element model of the bridge was generated using commercially available finite element analysis software using the elements provided. The model was analyzed with the help of CSi Bridge. In the current study, the field measurements captured and 3d element analysis performed for the concrete bridge composed of 9 supported spans in total 126.496m in length are presented. Static and dynamic tests on the existing bridge spans supported on abutments and piers with various lengths, and depending on these, a 3D computer model of the bridge generated using CSi Bridge software was calibrated through an optimization procedure, where the rigid bar lengths defined for the end parts of the bridge elements and spring constants were adjusted.

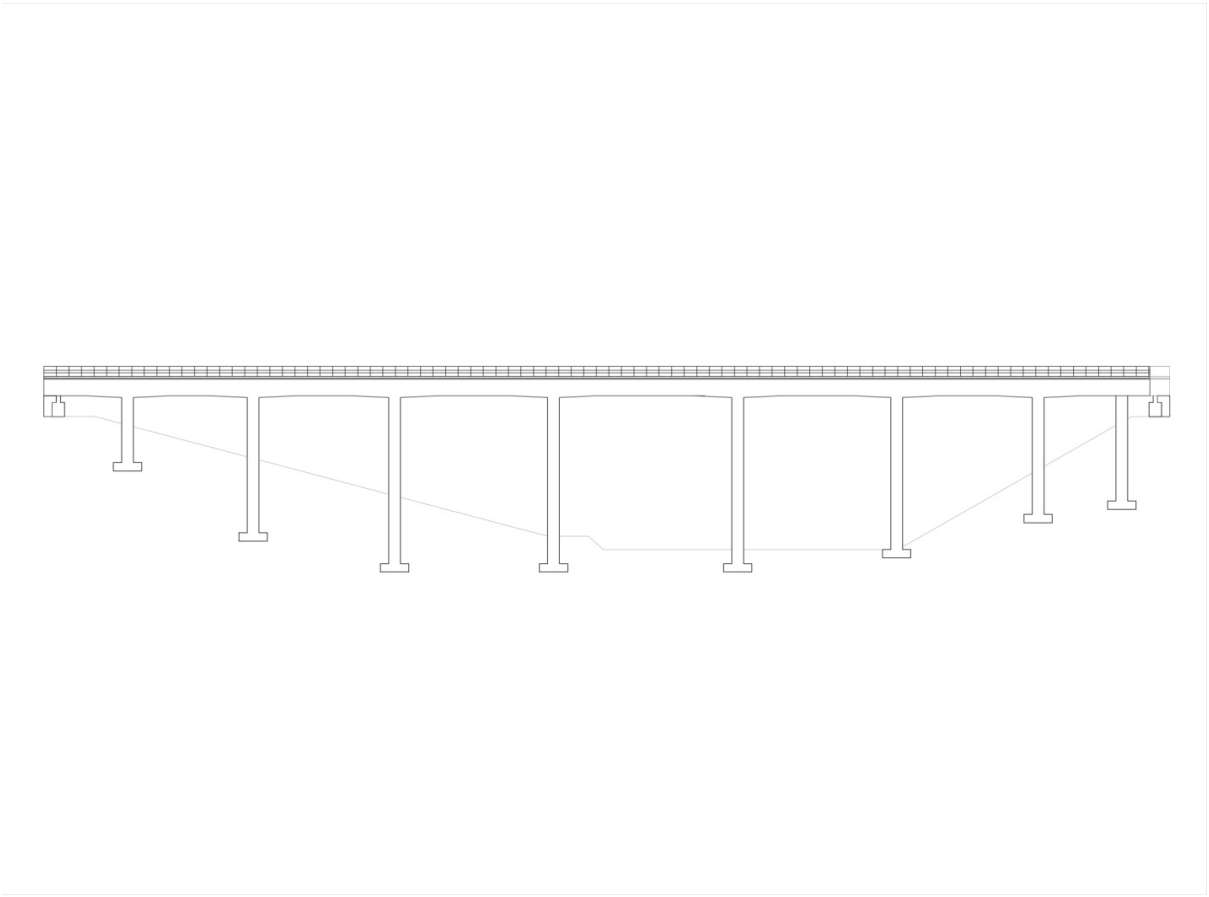

Figure 2: Bridge Elevation

1.1 Deck Elements

A continuous concrete girder box was used to model the deck. The deck was simulated to remain elastic during the analysis. This is a valid assumption because, to satisfy the appropriate strength and serviceability when vertical loads are applied. Decks usually have large cross sections that offer cogent strength against lateral bending. The deck does not include any intermediate hinges within. The reason of this limitation was to keep the computer model relative simple since the main subject of this paper is to analyze different scenarios and behaviors of the structure. Moreover, the given experimental data on the elastic behavior of simple hinges are not sufficient enough to allow for a more pragmatic hinge element model.

1.2 Pier Elements

Double-column piers were considered. The column elements were assumed to consist of a rigid top segment illustrating the distance from the deck centroid to the bottom of the deck. Nonlinear rotational springs are positioned at the base. The columns are simulated to be axially rigid. The reason of that is because axial forces on typical bridge columns are relatively small. The nonlinear spring at the base illustrates the length of part of the column where inelastic deformations happen. When a hinged detail is used at the bottom of the column, inelastic deformations will be restrained to the length of the hinge. The moment-rotation relationship for the elastic part and the rotational spring can be written as: (M. SAIIDIJ, . D. HART,and B. M. DOUGLAS, 1986)

Idealization of structural elements

Deck elements. A prismatic line element was used

$$\begin{Bmatrix} M_A \\ M_B \end{Bmatrix} = [K'] \begin{Bmatrix} v_A \\ \theta_B \end{Bmatrix} \quad (1)$$

1.3 Abutments

Two abutments represent the behavior of the boundary elements at each end of the deck. These boundary elements are designed to model the combined flexibility of deck-to-abutment detail as well as the flexibility of the abutment structure (effect of soil included) itself. In the case of using monolithic abutments in, the flexibility of springs is that of the abutment systems only. When the bridge deck is supported on soft bearings, the flexibility is overboard by that of the bearing system.

1.4 Pier Springs

Nonlinear springs model the foundation behavior at the base of the piers. The springs illustrate the displacement transverse to the bridge (z) as well as rotation about the bridge longitudinal axis (x). The rotation about the vertical axis was blocked in the model, even though it is a potential deformation when the bridge is loaded in the cross direction. This assumption was made due to the fact that the rotations are expected to be quite small.

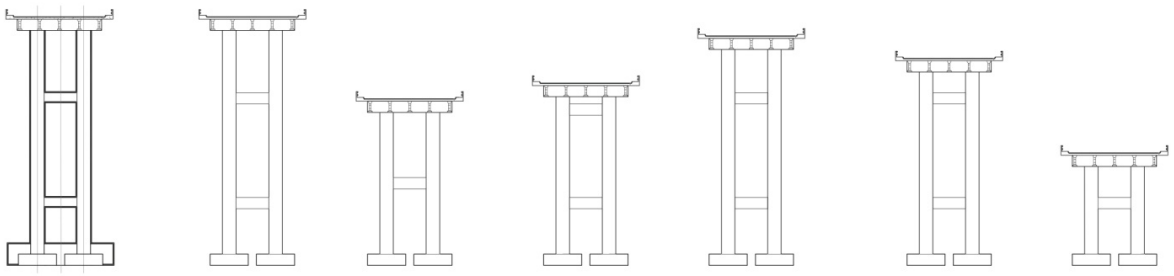

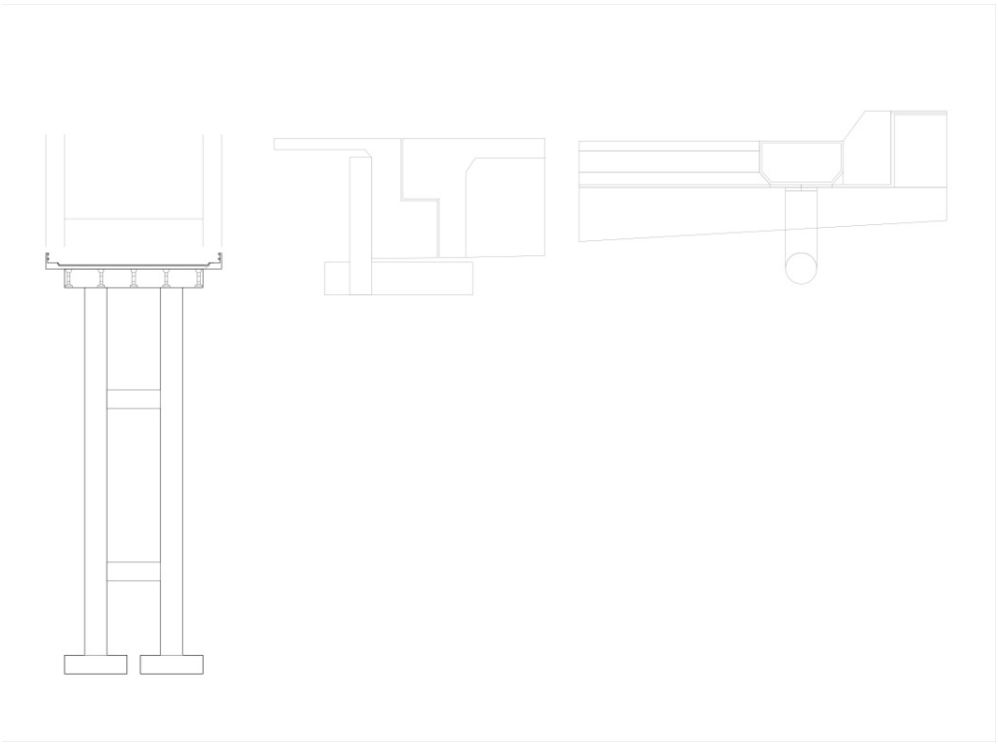

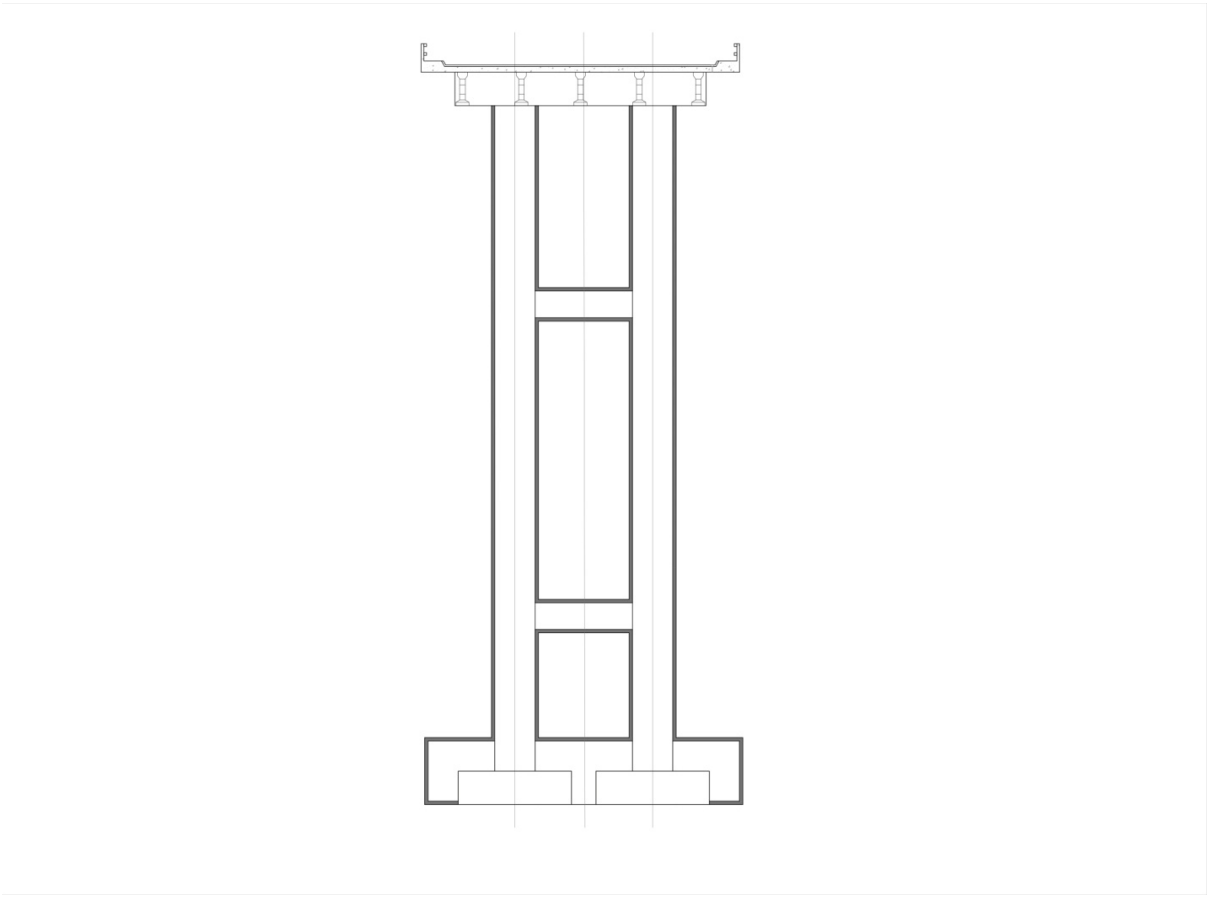

Figure 3: Bridge Piers

1.5 Analysis capapilities

The analytical model may carry out the following analyses:

(1) static analysis,

(2) free-vibration analysis,

(3) frequency analysis based on instantaneous stiffness,

(4) response spectrum analysis,

(5) modal analysis,

(6) creep and shrinkage.

The static analysis is implemented on the bridge model for transverse nodal loads occurred in single or multiple increments. The load sign can be varied for various load increments hence allowing for a cyclic load analysis of the bridge. The stiffness for the bridge elements is updated for every load increment.

The free-vibration analysis efficiency of the model was created for the analysis of experimental data occurred in the testing of the bridge. Free vibration is included in the analytical model by an imitative displacement and zero initial velocity.

The initiative displacement is created by static loads. These loads are removed analytically upon the beginning of free-vibration. The structural stiffness that is utilized at the beginning of free-vibration is the same one as the one at the end of the static loading. The stiffness for inelastic elements varies while the free vibration occurs, based on the regulations of the hysteresis models. The acceleration is simulated to remain constant over each time step.

Dynamic analysis (response spectrum and modal analysis) includes the calculation of vibration modes while using Ritz or Eigen vectors in order to find the natural vibration modes of the structure, which can be use for identifying the behavior of structure as well as the basis for modal superposition in the case of response spectrum and modal time history load. Ritz vector modal analysis reveals the optimum modes for obtaining structural behavior in response spectrum and modal time history load cases, in addition to the more efficient for this scope than Eigen-vector analysis.

Time dependent- creep and shrinkage analysis is focus on long term deflections of the bridge caused by the creep and shrinkage which can be illustrated along with staged sequential structural analysis.

The computational model is capable of estimating the frequencies as well as the mode shapes that will occur for the lateral modes of vibration. The accomplished stiffness of the structure is utilised in this computation. The reason of adding this capability in the model is to utilised the frequencies as an 'index' in order to illustrate the total stiffness modifications as a function of load amplitude.

2 Literature

2.1 Dead and Live Loads

The basic function of a bridge is to sustain traffic loads such as cars and heavy trucks. The responsibility of the engineer is to estimate the traffic loading that might be applied on the bridge. In the case of a short span bridge there is a possibility of conceiving the maximum load- on spans less than 30 metres long, four heavy trucks might cross at the same time, two in each direction of the lane. In the case of longer spans- thousand meters or more, the maximum conceivable load is a distant possibility. Therefore the engineers use possible loads as a basis for the bridge design. In order to carry the load of traffic, the structure must have some weight on its own, and on short spans this dead load weight is commonly less than the live loads. On longer spans, the dead load is much bigger than live loads and as spans gets longer, is eventually more essential to design forms that reduce dead load. Moreover, shorter spans are built with hollow boxes, arches, trussed, beams and continuous versions of the same while the longer spans use cable-stay, cantilever and suspension forms. As spans get longer the factors of form, materials and shape become increasingly essential. Advanced forms have evolved in order to provide longer spans with greater strength from less material.

Dead and Live loads are essentially occurred vertically, whereas natural forces may be either vertical or horizontal. Wind creates two important loads, one called dynamic and the other static. Dynamic wind load creates rise to a vertical motion, creating oscillations in any direction. Static wind load is the horizontal pressure that pushes the bridge sideways. Analogous to the breaking of an over-used violin string, oscillations are vibrations that are possible to damage the bridge (failure of bridge). If the deck surface is designed thin or not properly shaped and supported, it is possible to experience dangerous torsional (twisting) or vertical movements.

The contention and expansion of bridge components by heat and cold have been redused by the use of expansion joints in the deck with abutments and bearings at the top of piers. Bearings allow the bridge to response to different temperatures without causing damaging stress to the material. Modern bridges must as well resist natural disasters such as earthquakes, tropical and cyclones. Earthquakes are best withstood by structures that sustain

as light a dead load as possible because the horizontal forces that created from ground accelerations are proportional to the weigh of the structure.

2.2 Corrossion modelling

Damage modeling constitutes the devaluation of cross-sectional area of corroded bars, the devaluation of ductility of reinforcing steel and the corrosion of concrete strength due to splitting cracks, lamination and spalling of the concrete cover. Although corrosion does not have any impacts on the yielding strength of reinforcing steel bars (Apostolopoulos & Papadakis, 2008), a limited reduction of steel strength may appeared for corroded bars with discontinuous distribution of cross-section loss (Du, Clark, & Chan, 2005). This effect is not included in the applications situated in this paper, although it could be easily incorporated in the damage model. The damage of steel-concrete bond strength and the effects of the corroded steel bars are as well not investigated.

2.3 Effects of corrossion on concrete

The effects of deterioration are not limited to damage of reinforcing steel bars. Particularly in the case of uniform corrosion (Val, 2007), the formation of corrosion products may drive to the creation of longitudinal cracks in the concrete surrounding the corroded bars and, consequently, to lamination and spalling of the concrete surface. This local corrosion of concrete can effectively be modeled by means of a degradation law of the effective resistant area of the concrete matrix $\mathbf{A_c}$ (Biondini et al., 2004):

$$A_c = [1-\delta_c(\delta)]\, A_c0$$

Where Ac0 is the field of undamaged concrete and $\delta_c = \delta_c(\delta)$ is a dimensionless deterioration function which gives the number of concrete damage in the range [0;1]. Nonetheless, in this form, it may be not straightforward to create a relationship between the damage function δ_c and the corrosion penetration index δ. The effects of concrete deterioration can be taken into account by modeling the decrease of concrete compression strength fc due to longitudinal cracking (Biondini & Vergani, 2012):

$$f_c = [1- \delta_c(\delta)]\, f_{c0},$$

Where f_{c0} is the strength of undamaged concrete. The reduced concrete strength f_c can be evaluated as follows (Coronelli & Gambarova, 2004):

$$f_{c=},$$

in which κ is a coefficient related to bar diameter and roughness (κ = 0.1 for medium-diameter ribbed bars), εc0 is the strain at peak stress in compression and is an average (smeared) value of the tensile strain in cracked concrete at right angles to the direction of the applied stress.

The transversal strainis evaluated by means of the following relationship:

$$\varepsilon_{\perp} = \frac{b_f - b_i}{b_i} = \frac{\Delta b}{b_i},$$

Where bi is the width of the undamaged concrete cross-section and bf is the width after deterioration cracking. The increase of beam width Δb can be estimated as follows (Biondini & Vergani, 2012):

$$\Delta b = n_{\text{bars}} w,$$

Where nbars is the number of steel bars and w is the average crack opening for each bar. Several studies investigated the relationship between the amount of steel corrosion and the crack opening w (Alonso, Andrade, Rodriguez, & Diez, 1998; Zhang et al., 2009). The following empirical model is assumed (Vidal et al., 2004):

$$w = \kappa_w(\delta_s - \delta_{s0})A_{s0},$$

In which kw =0.0575 (mm^{-1}) and δs0 is the amount of steel damage necessary for cracking initiation. This damage threshold is evaluated as follows:

$$\delta_{s0} = 1 - \left[1 - \frac{R}{D_0}\left(7.53 + 9.32\frac{c_0}{D_0}\right) \times 10^{-3}\right]^2,$$

Where Co is the concrete cover. The crack opening w increases with the expansion of corrosion products up to a critical width wcr which corresponds to the occurrence of delaminating and spalling of the concrete cover. Based on experimental evidence, delaminating and spalling can occur for crack width in the range 0.1–1.0mm (Al-Harthy, Stewart, & Mullard, 2011; Torres-Acosta & Martinez-Madrid, 2003; Vu, Stewart, & Mullard, 2005). The reduction of concrete strength is generally applied to the entire concrete cover (Coronelli & Gambarova, 2004).

Nonetheless, the longitudinal cracks pattern mostly depends on the organization of reinforcing bars. Cracking propagation persuaded by corrosion should be therefore restrained to the zones adjacent to the corroded bars. Figure 4 shows a model where the reduction of concrete strength is applied only to a portion of concrete cover surrounding the corroded bars (Biondini & Vergani, 2012).

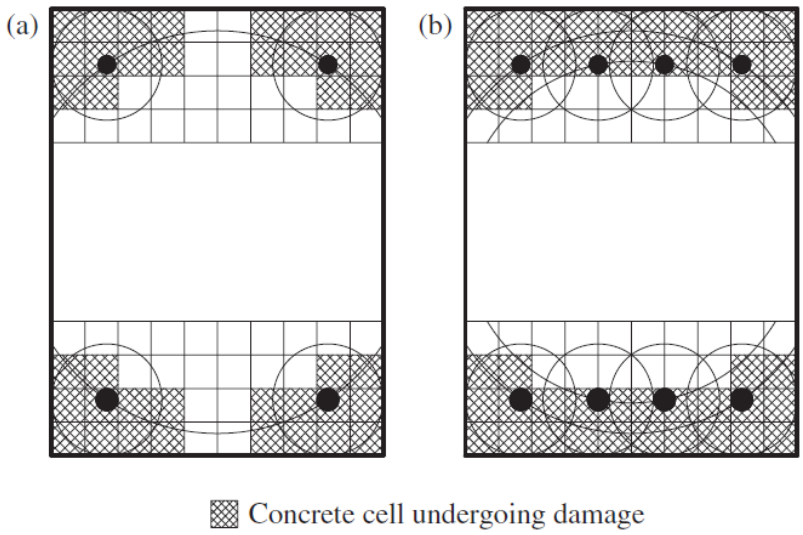

Figure 4: Corrosion on concrete

The rectangular cross-section is sub-divided in cells and each concrete cell in the neighborhood of a damaged bar is assigned to deteriorate if at least one of its vertices lies in the intersection of the area surrounding the bar inside a radius that is equivalent to the cover thickness and they are outside the censorial circle passing through the bar. This model allows to successfully reproducing the mechanism of spalling of the concrete cover, described by inclined fracture planes for wide bar spacing [see Figure 4(a)] as well as parallel fracture planes for closely spaced bars [see Figure 4(b)].

2.4 Analytical Models

Most commonly used analytical models for reduplicate concrete cover cracking due to deterioration of the reinforcement bars are based on the thick walled cylinder approach. According to figure 5 the interior circular boundary at the interface of reinforcement and concrete is displaced to contain the expansive corrosion elements. The primary radius of the reinforcement bar is R_i and $_c$ is the clear cover of concrete to the reinforcement. R_c illustrates the radius of the crack at which the tensile capacity of the concrete is achieved. Since R_c becomes R_{i+c}; the cover of concrete is considered to be fully cracked. According to Liu and

Weyers, a so-called ‘‘porous’’ zone of finite thickness do around the reinforcement bar is included to account for voids at the interface steel–concrete that allow first diffusion of corrosion products with no contribution to the pressure exerted on the concrete.

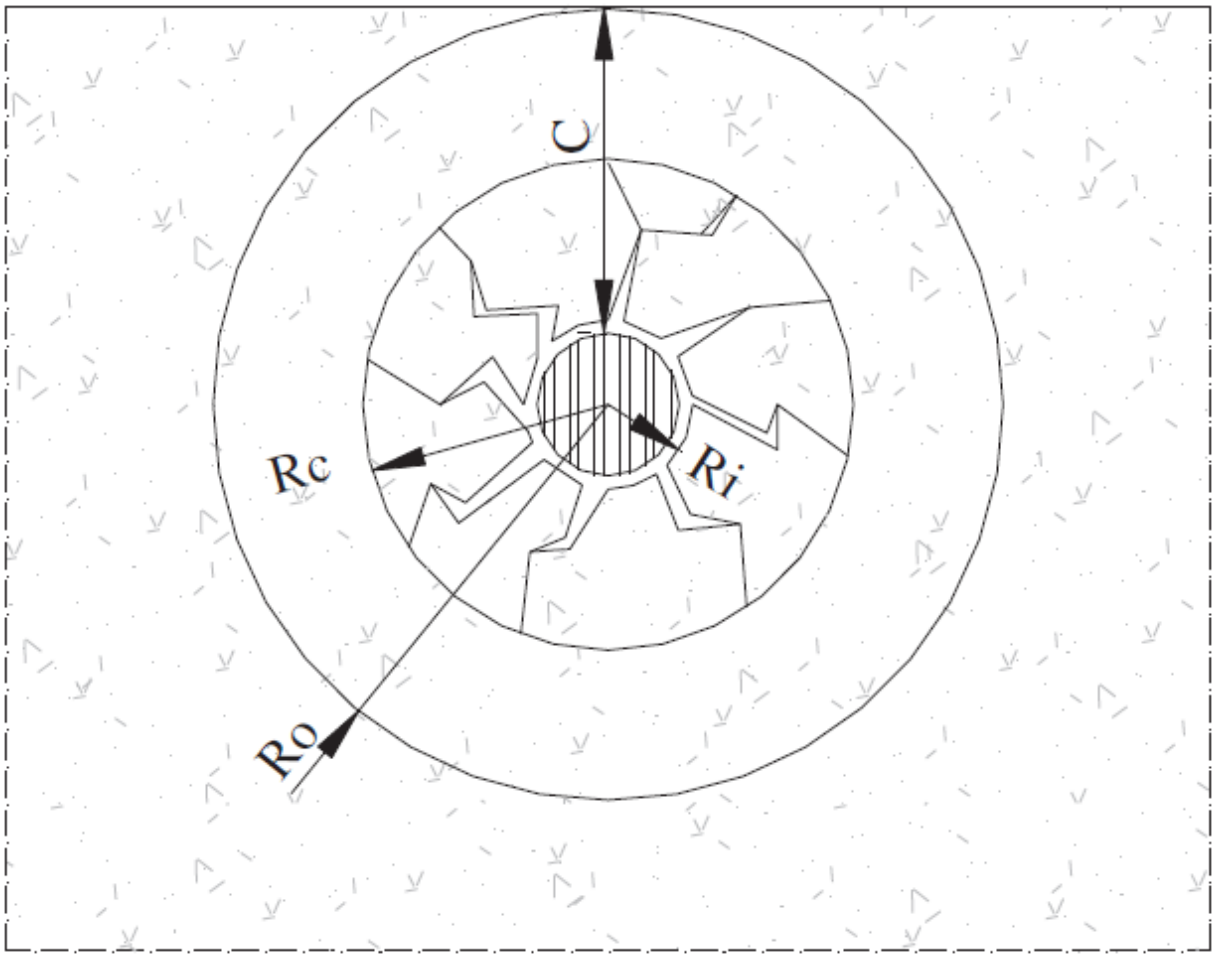

Figure 5: Concrete corrossion elements

2.5 Seismic analysis

Reinforced concrete bridge columns are assigned not only to vertical loading effects occurring from gravity, but in addition to combined variable axial forces, shear and moment resulting to actions such as earthquake loading. Because of the ‘lateral moment’, columns in multi-column cross-heads are subjected to variable axial forces responding to the direction of the lateral forces. The behavior of a reinforced concrete column under variable axial load is

different fundamentally from that of reinforced concrete bridge column under the effect of constant axial load. Seismic performance of a reinforced concrete bridge column, in particular, designed according to constant axial load with a relatively small axial load ratio, may not satisfy the requirement performance when the definite axial load owing to the lateral moment results in multicolumn cross-heads or the vertical ground motion surpasses the demand axial load. The result of variable axial forces evolves into more importantly when the shear strength of the concrete bridge columns is considered. An immediate variation of axial force form compression to tension can importantly reduce the shear strength of the reinforced concrete column of the bridge. Regardless of the serious effects of variable axial forces on the seismic realization of the reinforced concrete bridge columns, just a few researches have experimentally studied these results and the majority of the previous experimental tests have been operated on reinforced concrete bridge columns under different axial loads. Recently, several analytical works have considered the results of variable axial loads proportional to the moment from lateral force on the seismic reaction of reinforced concrete bridge columns.

2.6 Modal Parameters

Until now, only a few studies have investigated the result of damage on modal parameters of full scale concrete bridges. Kato and Shimada in 1984 studied the changes of several natural frequencies while failure tests of a reinforced concrete bridge. The essential effect was the decrement of natural frequencies because of cracks in concrete, was small as long as the steel wasn't exceeding the yield stress. Since this stress was exceeded an immediate decrement of natural frequencies was investigated. Toksoy and Aktan in 1994 accomplished modal testing on a constant three span reinforced concrete slab bridge which was loaded up to failure. The researchers reported that natural frequencies, modal damping as well as mode shapes could not accurately identify the location and level of damage. Better damage identification results were achieved by applying the modal flexibility matrix. Catbas et al. in 1997 utilised modal testing for damage identification on a three span steel stringer bridge. The bearing plates removal was located successfully by using the modal flexibility of the bridge. The size of the damaged was calculated by evaluating measured deflections of heavytrucks loading tests. A few damage assessment methods were compared in Farrar and Jauregul in 1998 using experimental modal data resulting from tests on the incrementally deteriorated i40 Bridge; a

bridge setup of a concrete deck sustained by welded steel plate girders and steel stringers. The outcomes confirm, in agreement with the previous studies, that natural frequencies and mode shapes are weak indicators of damage. A refined ability to identify damage of most uncompromising damage cases was achieved by applying more sophisticated damage identification methodology. Nevertheless, ambiguous results were achieved for less uncompromising damage cases. According to the damage cases performed on the z24 bridge, a three span concrete bridge, Kraemer et al.1999; Maeck and De Roeck 2003 stated that natural frequencies and mode shapes are appropriate indicators for the development of severe damage, given that the cracks in concrete still are open. Nevertheless the performed damage scenario, adjustment of a pier, created in a small part of the superstructure on a small area, concentrated cracks that were open while the modal analysis tests were running. The location and the amount of damage of the most rigid damage case were successfully assessed using the direct stiffness estimation method. The researchers stated an almost full recovery of stiffness after covering of cracks. The recovery of the stiffness made more complicate the detection of the damaged based on modal parameters. In order to study the accuracy of an early stage assimilation of damage in prestressed bridges according on modal parameters as well as to extent experiences in this area of study, full scale tests on concrete highway bridge have been achieved. The accomplished damaged scenarios given distributed cracks in the superstructure. The modal analysis investigations were applied after un-loading of the super structure whereas the cracks almost entirely closed.

2.7 Creep effect

Creep effect may have significant influence on the structural configuration and interior force distribution, particularly when the structural system and configuration varies during construction. As long as the concrete stress during service is below 50% of its compressive strength, the linear creep model is often adopted in creep analysis. In the case of non linear analysis the creep effect will expected to interact with such non linear behavior as the crack of concrete and so on. Furthermore, due to presence of the reinforcement or prestress tendon will occur. Because of the degenerated beam element is adopted, the communication between the creep and nonlinear material behavior as well as the effect of the reinforced tendon can be managed with conveniently. In past studies, numerous methods including effective modulus,

rate of flow, rate of creep, dischinger method and trost bazant method are used to investigate the creep effect.

2.8 CSi Model Analysis – Loads effect

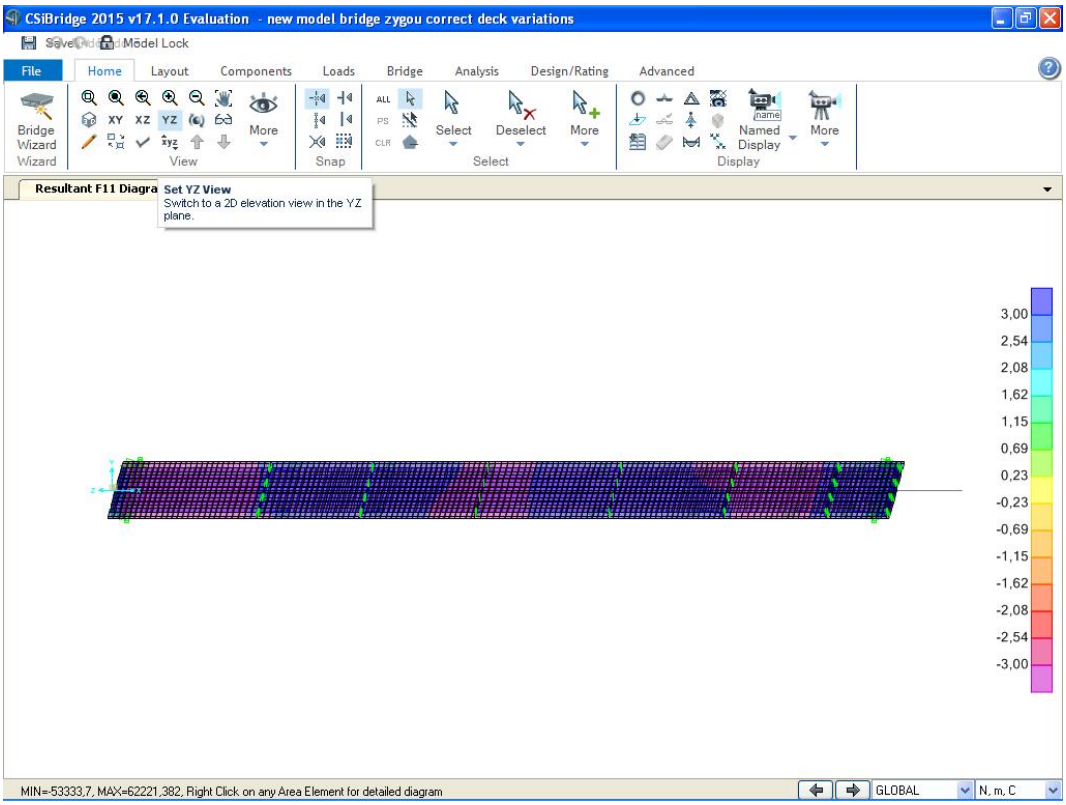

Figure 6: Trucks Load

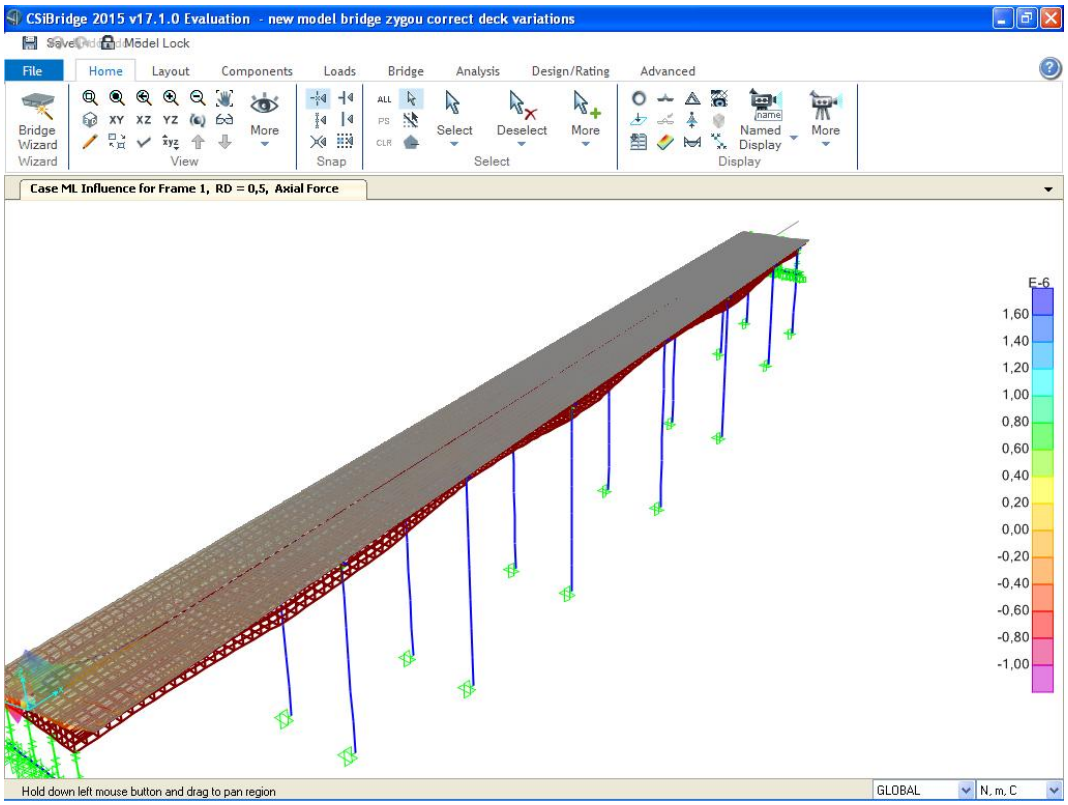

Figure 7: Axial Force

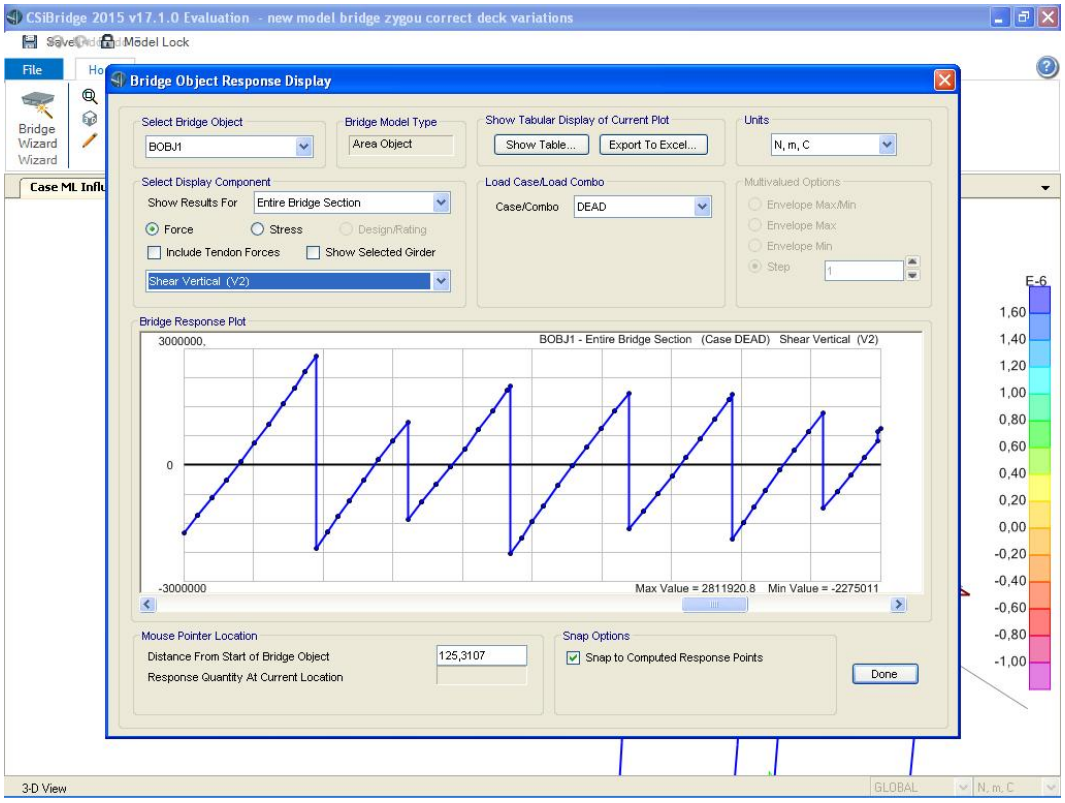

3 Analysis – Damage Scenarios

3.1 Direct Stiffness Calculation

The Direct Stiffness calculation applies the investigational eigen-frequencies and mode-shapes in obtaining the dynamic stiffness. The process applies the basic relation that the dynamic bending stiffness *EI* in each part is even to the bending moment *M* in that part separated by the equivalent curvature (2nd imitative of bending mode φb).

1

$$EI = \frac{M}{\mathrm{d}^2\varphi^b/\mathrm{d}x^2}.$$

First the moment in each part of the structure has to be resolved. The eigen-value problem for the dry system can be described as:

2

$$K\varphi = \omega^2 M\varphi$$

In which *K* describes the stiffness matrix, *M* is the mass matrix, ω the measured eigen-pulsation and φ the measured mode-shape. This can be pursued as *pseudo static* system: for every mode internal section forces are the consequences of inertial

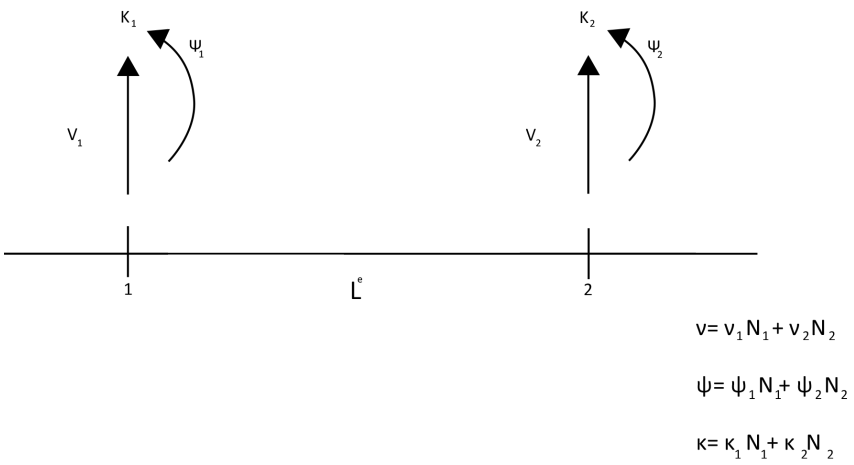

Figure 8: Finite element variables

forces that can be measured as the creation of local mass and local acceleration [= ω2φ]. The mass spreading is assumed to be as a given. A piece of mass matrix is used in $K\varphi = \omega^2 M\varphi$. The density of the measurement mesh is acceptable. To measure the modal internal forces needed to estimate equation 1, the static analysis with the *pseudo static* forces from the equation 2 as load has to be transferred out – for example with a finite element package.

The next stage in obtaining the dynamic bending stiffness is formed by the calculation of the curvatures along the beam for every mode-shape. To calculate the curvatures from the estimated mode-shapes is through using the main difference approximation outcomes in inaccurate values. A smoothing process that accounts for the intrinsic inaccuracies of the calculated mode-shapes, should be applied. Consequently, a weighted remaining penalty based technique is implemented which is similar to the finite element approach. The structure is separated into numerous elements divided by nodes that indicated to the measurement points.

Every node has three degrees of freedom: the rotation ψ, the curvature κ and the modal displacement v_a , which are estimated independently figure .. Linear shaped function N_i are used. The method is equivalent to the Mindlin plate element, for which the rotations are estimated independently from the bending deflection.

The aiming function contains the difference between the estimated and calculated mode-shapes. Two penalty conditions are added to help the continuity of rotations and curvatures in an indicate smudge way where φ_m denotes the calculated mode-shape, and L_e is the length of a finite element. Elements are selected in a specific way that nodes match with measurement points. The first term described that the average variation between estimation and measurement has to be minimized.

3
$$\pi = \int \frac{(v-\varphi_m)^2}{2}\,\mathrm{d}x + \frac{\alpha L^{e2}}{2}\int\left(\psi - \frac{\mathrm{d}v}{\mathrm{d}x}\right)^2 \mathrm{d}x + \frac{\beta L^{e4}}{2}\int\left(\kappa - \frac{\mathrm{d}\psi}{\mathrm{d}x}\right)^2 \mathrm{d}x$$

In order to attain a filtering of investigational errors and so an uninterrupted of the deflection, two extra terms are added. Variations are minimized between the sufficient approximations of rotations and curvatures with the initial imitative of displacements and rotations. The combination between the independently estimated unknowns is set by these constrain conditions. The weight of these further conditions is established by the dimensionless penalty aspects α and β.

Obtaining 3 to the unidentified variables ν, ψ and κ assigns a system of dimension three times the number of nodes. As α and β are penalty conditions they are known in the system but should be chosen by the user. The advantages of the Mindlin method are that curvatures are obtainable which boundary conditions be imposed simply and which the estimated modal deflections do not have to go through all calculated points. The disadvantage is that penalty features must be selected in a permissible range: considerable enough to be effective and not too large to evade numerical difficulties. The direct stiffness measurement operates the experimental mode-shapes in obtaining the dynamic stiffness. For hyperstatic systems the reaction and internal forces are sustained on the stiffness of the structure. As a result of an iterative process is required to find the EI spreading of the structure.

3.2 Seismicity and structural demand

The LCC (Life-Cycle Cost) analysis involves first to calculate the seismic characteristics of the area (eg earthquake sources and rates of occurrence). This section shows the probabilistic model operated in the presented methodology to simulate the occurrence and the magnitude of the earthquakes. Additionally this section expresses the computation of structural parameters such as seismic energy as well as numerous of inelastic cycles of the reaction of an equivalent single degree of freedom system.

3.2.1 Seismicity modeling and calculation of ground motion parameters

The moment magnitude, M_w is used to describe the strength at the source of an earthquake. Magnitudes are labeled independently of the time of the event of each earthquake applying a cumulative separation function derived from the relationship of frequency –magnitude

provided by Gutenberg and Richter as:

$$N_{\mathrm{eq}}(M_{\mathrm{w}}) = 10^{a-bM_{\mathrm{w}}}$$

Where $N_{eq}(M_w)$ describes the cumulative annual percentage of earthquakes with magnitudes larger than M_w as well as and b are dimensionless parameters that rely on the area seismicity. The obtained sampling separation is then:

$$F(M_{\mathrm{w}}) = 1 - \frac{10^{a-bM_{\mathrm{w}}}}{10^{a-bM_{\mathrm{w,min}}}}$$

Where M_{wmin} describes the smallest possible magnitude or earthquakes for the selected area. The result of earthquakes is modeled as a Poisson's method with a mean value appropriate for the area. The Poisson distribution is described as:

$$f(x) = \frac{(v)^x}{x!}\exp(-v)$$

Where *x* describes the number of the event of an earthquake in the time window T_H, which is the time span over that LCC is computed, ν describes the number of earthquake events T_H, and f(x) is the possible density function (PDF) of x. In Poissons method the time intervals between two events follow an exponential allocation. Consequently, the time of events of (M+1) the earthquake is described as follows:

$$t_{M+1} = t_M + \Delta t, \quad M = 1, 2, 3, \ldots$$

Where t_M illustrates the time of the event of the Mth earthquake and Δ_t illustrates the time interval between two earthquakes imitated using the PDF below:

$$f(\Delta t) = \left(\frac{v}{T_H}\right) e^{-(v\Delta t/T_H)}$$

The top ground acceleration A_H and top ground velocity V_H at the site of the bridge are calculated by the ground motion attenuation relationships as provided by Campbell. The attenuation connection for A_H is described as:

$$\begin{aligned}\ln(A_H) = {} & -3.152 + 0.904 M_w - 1.328 \ln\sqrt{R_{SEIS}^2 + [0.149 \exp(0.647)]^2} \\ & + [1.125 - 0.112 \ln(R_{SEIS}) - 0.957 M_w] F \\ & + [0.440 - 0.171 \ln(R_{SEIS})] S_{SR} + [0.405 - 0.222 \ln(R_{SEIS})] S_{HR} + \varepsilon_A\end{aligned}$$

Where R_{SEIS} describes the distance of the origin from the site of the bridge, F is an index variable applied to indicate the style of faulting, S_{HR} and S_{SR} are index variables that illustrate the local site conditions. ε_A describes the model error which is modeled as a random variable having normal allocation with mean of zero and standard divergence provided by the equation below:

$$\sigma_A = \begin{cases} 0.889 - 0.0691 M_w, & M_w < 7.4 \\ 0.38, & M_w \geqslant 7.4 \end{cases}$$

The attenuation relationship is given by:

$$\begin{aligned} \ln(V_H) = {} & \ln(A_H) + 0.26 + 0.29 M_w - 1.44 \ln[R_{SEIS} + 0.0203 \exp(0.958 M_w)] \\ & + 1.89 \ln[R_{SEIS} + 0.361 \exp(0.576 M_w)] \\ & + (0.0001 - 0.000565 M_w) R_{SEIS} - 0.12 F - 0.15 S_{SR} - 0.30 S_{SR} \\ & + 0.75 \tanh(0.51 D)(1 - S_{HR}) + f_v(D) + \varepsilon_V \end{aligned}$$

Where ε_V is again the model inaccuracy modeled as a normal unsystematic variable with zero mean and typical deviation given by the following:

$$\sigma_V = \sqrt{\sigma_A^2 + 0.06^2}$$

The function $f_{v(D)}$ is given as:

$$f_v(D) = \begin{cases} 0, & D \geqslant 1\,\text{km} \\ -0.30(1 - S_{HR})(1 - D) - 0.15(1 - D) S_{SR}, & D < 1\,\text{km} \end{cases}$$

Where D describes the depth to the base from the ground level at the bridge site.

3.2.2 Cumulative seismic damage

When it comes to earthquake loading, bridge columns experience several cycles of inelastic divergences. Consequently low cycle fatigue analysis is applied in this research to estimate the seismic damage. Moreover, an estimated strength degradation equation suggested by Das is applied to calculate the structural properties of the contaminated structure. This part first illustrates the background and the process implemented to model the low cycle fatigue. Furthermore the calculation of the damage index (DI) is analysed. Lastly the methodology to calculate structural properties of a damaged structure is presented.

3.2.2.1 Low-cycle fatigue

Based on Coffin and Manson theory of fatigue formulates the reaction of longitudinal bars under reversed cyclic loading as:

$$\varepsilon_p = \varepsilon_f'(2N_f)^c$$

Where ε_p describes the plastic strain amplitude, ε_f and c describe the material constants given experimentally; 2N is the number of half-cycles for the 1st fatigue crack on the longitudinal support bar.

Mander, achieved the following equation for ε_p based on experiments on supporting bars:

$$\varepsilon_p = 0.08(2N_f)^{-0.5}$$

Likewise, Kunnath achieved the following expression:

$$\varepsilon_p = 0.065(2N_f)^{-0.436}$$

Tsuno and Park developed Mander and Kunnaths theory of damage models further by carrying out an experimental work. They tested five *RC* columns with various loading patterns and compared the observed damage with the damage predicted. It was observed that the model of Kunnaths predicts the failure well for the *RC* columns that are designed seismically according to Caltrans or *AASHTO* in order to have a dominant flexual damage mode. Kunnaths model was established on experiments on RC columns and therefore accounts for damage in columns as a composite of steel and concrete. Mander's model was established on eperiments on steel reinforcement columns and accounted for damage in steel only. Neverheless, the drawback on Kunnath's model is that it underestimates the damage when it comes to the case of extreme loading cases that have large displacements in the first cycle. The model established by Mander found to be more accurate in the case of extreme loadings than Kunnaths model. In this examination, instead of the connection between ε_p and N_f the use of modification for the relation suggested by Kunnath and Chai is applied to model the low-cycle failure behavior for circular ductile RC columns as stated below:

$$U_{yM}^{+} = U'_{yM} + \sum_{N=1}^{M-1} \Delta U_{yN}, \quad M = 2, 3, 4, \ldots$$

$$\Delta U_{yN} = U_{yN}^{+} - U_{yN}^{-}$$

Where U'_{yM} describes the displacement at time tM caused to the corrosion only. Figure 7 evaluates the contributions of the cumulative seismic damage as well as corrosion in the deterioration of the bridge model example.

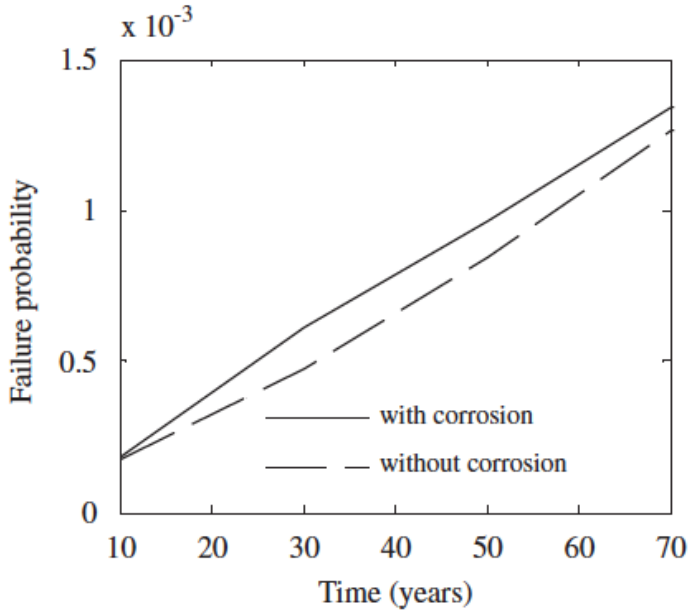

Figure 9: Failure probability / Time

3.2.2.2 Cumulative DI

Applying Miner's rule, the cumulative DI can be calculated as follows:

$$\mathrm{DI} = \sum_{j=1}^{m} \frac{1}{2N_{\mathrm{f}j}}$$

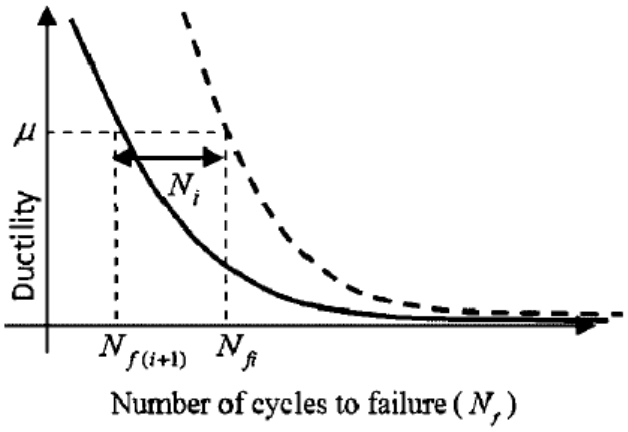

Figure 10: Updating fatigue curve

Where DI describes the cumulative DI after m half cycles, N_{fj} describes the number of cycles to failure equivalent to the displacement in j the half cycle of loading. Equation can be modified to calculate the cumulative seismic Di as follows:

$$\mathrm{DI}_M = \frac{N_M}{N_{\mathrm{f}}M} + \mathrm{DI}_{M-1}, \quad M = 2, 3, 4, \ldots$$

Where N_M describes the corresponding number of continuous amplitude inelastic cycles in the Mth earthquake calculated using the equation $N = \frac{\alpha E_{\mathrm{I}}}{4\alpha_{\mathrm{h}} V_{\mathrm{y}} U_{\max}}$ and N_{fM} describes the number of cycles to damage for the peak displacement of Mth earthquake calculated with $N_{\mathrm{f}} = \left(\frac{c_1}{\mu}\right)^{c_2}$ Based on Miner's theory, failured is supposed to occur when DI >_1.0.

3.2.2.3 Structural properties of damaged stucture.

The structural properties x_p of an immaculate bridge are described as follows:

$$x_p=(k,T,Uy,Vy)$$

Where k described the lateral column stiffness.
Due to structural damage, it is possible that the stiffness of the column, k, decreases due to each has experienced earthquake. The cyclic loading, while each earthquake also effects in the failure of the bond between concrete and steel, that results in a larger displacement at yield U_y. Das proposed that the following equations (i and ii) account for the changes in the stiffness as well as the displacement at yield owing to an earthquake.

$$k_M^+ = k_M^- \left[1 - \frac{U_{\max M} - U_{yM}^-}{U_u - U_{yM}^-}\right]^{0.1}, \quad M = 1, 2, 3, \ldots$$

i

$$U_{yM}^+ = \left[\frac{k + k_M^-}{k + k_M^+}\right] U_{yM}^-, \quad M = 1, 2, 3, \ldots$$

ii

Where k-M and k+M describe column stiffness before and after Mth earthquake. The number U_u is the maximum displacement under the monotonic loading of the immaculate column. The yield displacement $U+_{yM}$ after Mth earthquake is provided by the equation ii. Where k describes the immaculate column stiffness. As predictable, these equations represent that the earthquake loading reduces the column stiffness as well as increase the displacement at yield. The terms of $T+_M$ and V+ can be described by the following:

$$T_M^+ = 2\pi\sqrt{\frac{m}{k_M^+}}, \quad M = 1, 2, 3, \ldots$$

$$V_{yM}^+ = k_M^+ U_{yM}^+, \quad M = 1, 2, 3, \ldots$$

3.2.2.4 Life-cycle cost analysis

The Life-cycle cost of a structure is described as the overall cost that is incurred, during its life-cycle. LCC analysis offers a framework to give decisions about resource allocation linked to the design, operation and construction (inspection and maintenance). Various

formulations for the LCC can be obtained, eg by including multiple limit states or allowing several hazards. Following Wen and Kang as well as Kong and Frangopol, the estimated LCC of a structure is described mathematically as stated below:

$$E[LCC(p)]= E[C_C(p)+NPV(C_M(p), t)+NPV(C_{IN}(p), t)+NPV(C_F(p), t)]$$

Where C_C describes the initial construction cost, C_{IN} the cost of inspections, C_M the maintenance cost, C_F the failure costs, E [.] implies the expectation operator. Vector p=a illustrates the decision variables that include factors such as design criteria and inspection and maintenance schedules. The net shows

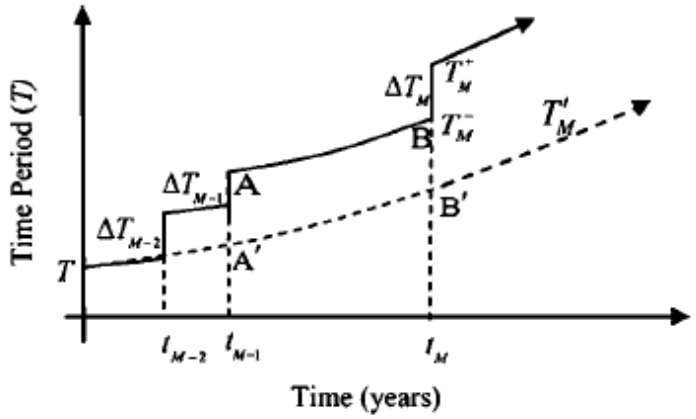

Figure 11: Deterioration in period due to earthquakes and corrosion

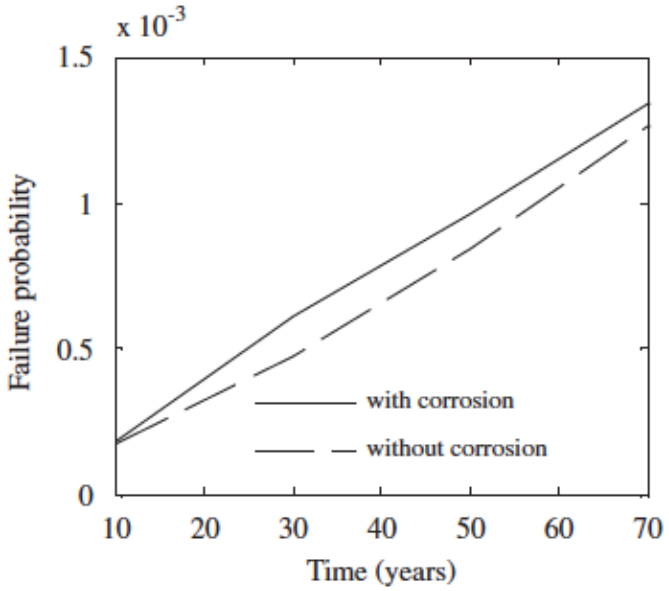

Figure 12: Effect of cumulative seismic damage on annual failure probability.

value is applied to discount the cost and to compose decisions at time t=0.The net value of cost – C is uncured at time t and is calculated as

$$\mathrm{NPV}(C,t)=\frac{C}{(1+r)^t}$$

Where r describes the discount value.

3.2.2.5 Expected Life-Cycle Cost

The Expected Life-cycle cost can be described by the following equation:

$$E[\mathrm{LCC}(\mathbf{p})]=C_{\mathrm{C}}(\mathbf{p})+E\left[\sum_{i=1}^{m(T_{\mathrm{H}})}\frac{(C_{\mathrm{C}}(\mathbf{p})\Delta P_{\mathrm{f}}(\mathbf{p},t)+C_{\mathrm{IN}}(\mathbf{p}))}{(1+r)^{t_i}}\right]+\int_0^{T_{\mathrm{H}}}\frac{2C_{\mathrm{C}}(\mathbf{p})}{(1+r)^t}P_{\mathrm{f}}(\mathbf{p},t)\,\mathrm{d}t$$

3.2.2.6 Data analysis using CsiBridge

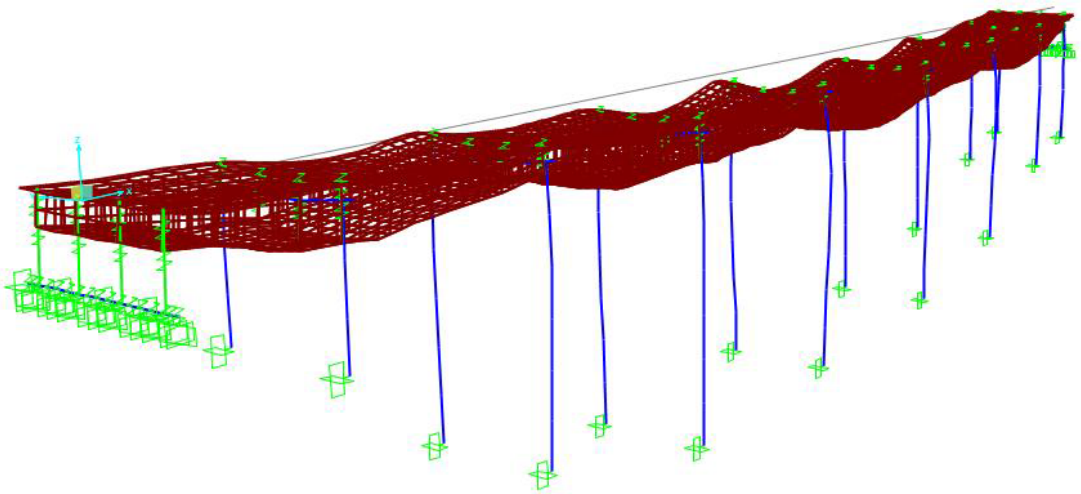

Figure 13: Deformed shape/ GRAV

Mode	Calculated Freq.Hz	T	MAC	Mode type	Measured Freq.Hz (from existing ZB)	UY
1	0,60327	1,65764	---	Lateral	0,60	
2	2,87021	0,34841	---	Torsional	---	
3	4,08294	0,24492	---	Longitudinal	4,30	
4	4,08940	0,24453	---	Lateral	---	
5	4,15748	0,24053	---	Longitudinal	4,52	
6	4,21687	0,23644	---	Longitudinal	4,50	
7	4,26734	0,23198	---	Lateral	---	
8	4,31638	0,22732	---	Longitudinal	---	
9	4,35488	0,22389	---	Longitudinal	---	

Table I: Measured and numerical parameters for bridge example model on CsiBridge

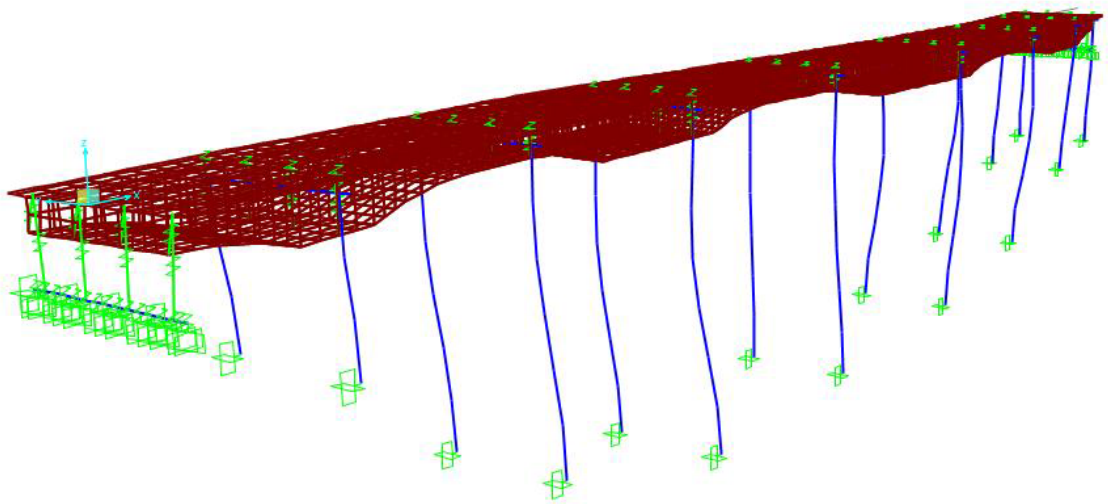

Figure 14: Deformed shape/ mode 1

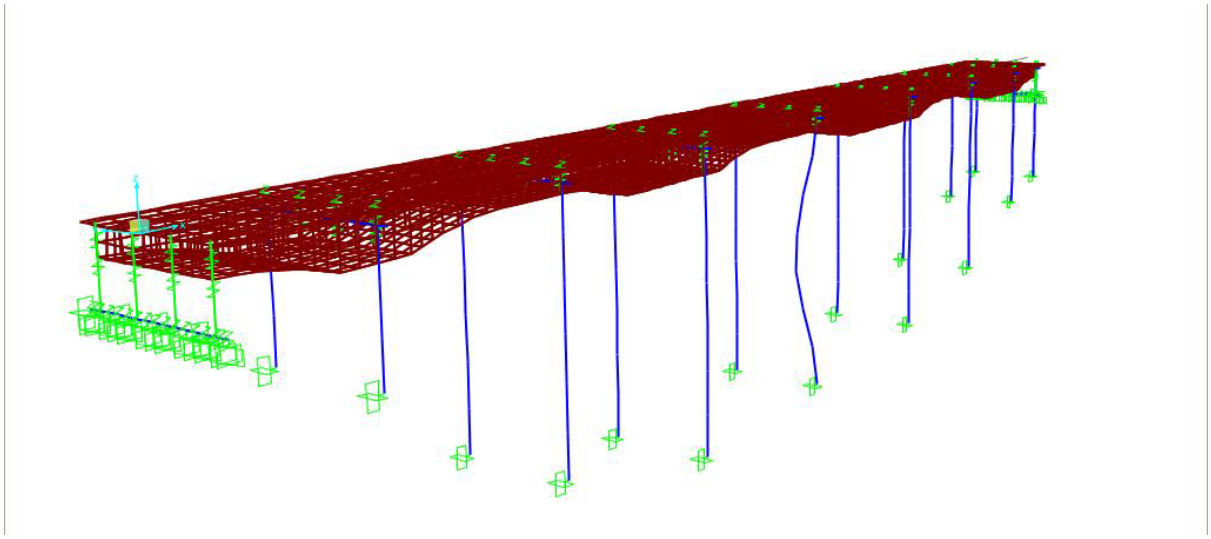

Figure 15: Deformed shape/ mode 2

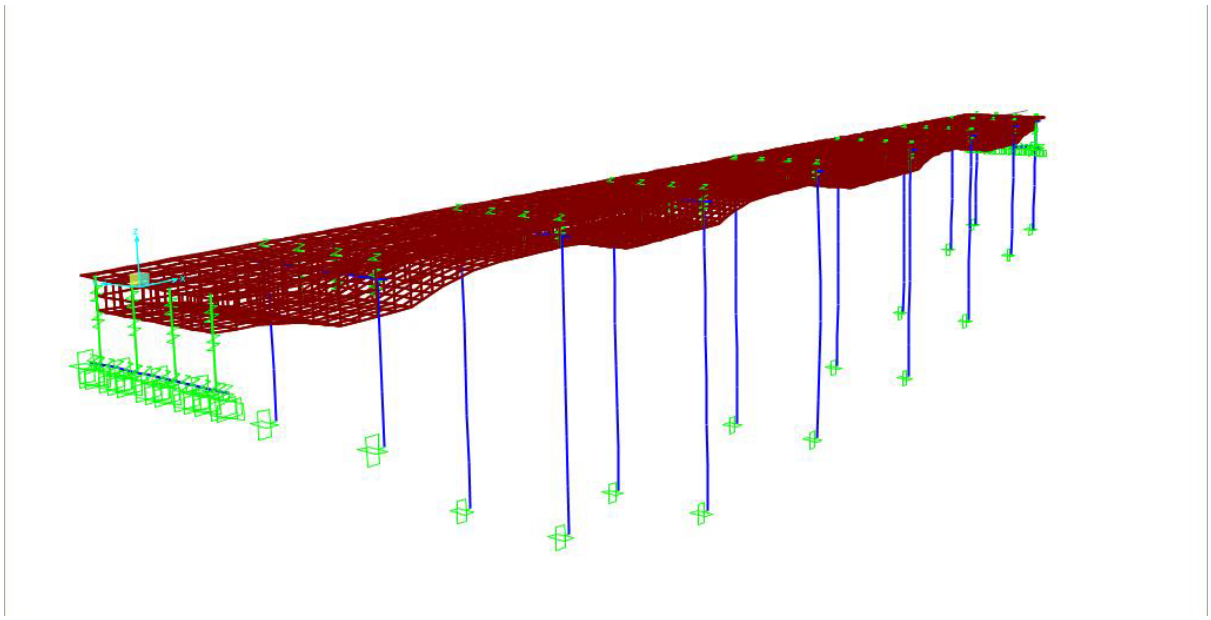

Figure 16: Deformed shape/ mode 3

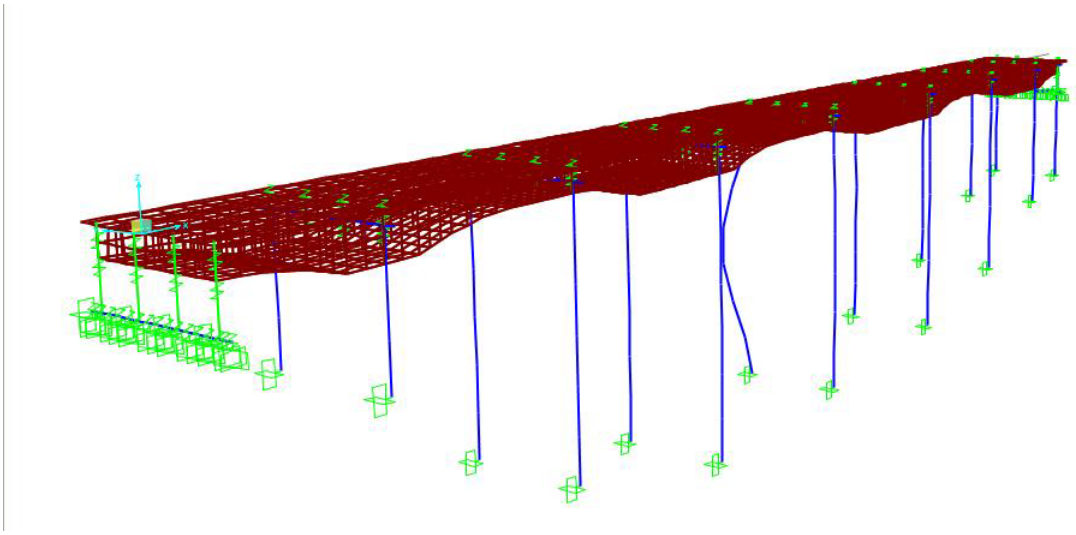

Figure 17: Deformed shape/ mode 4

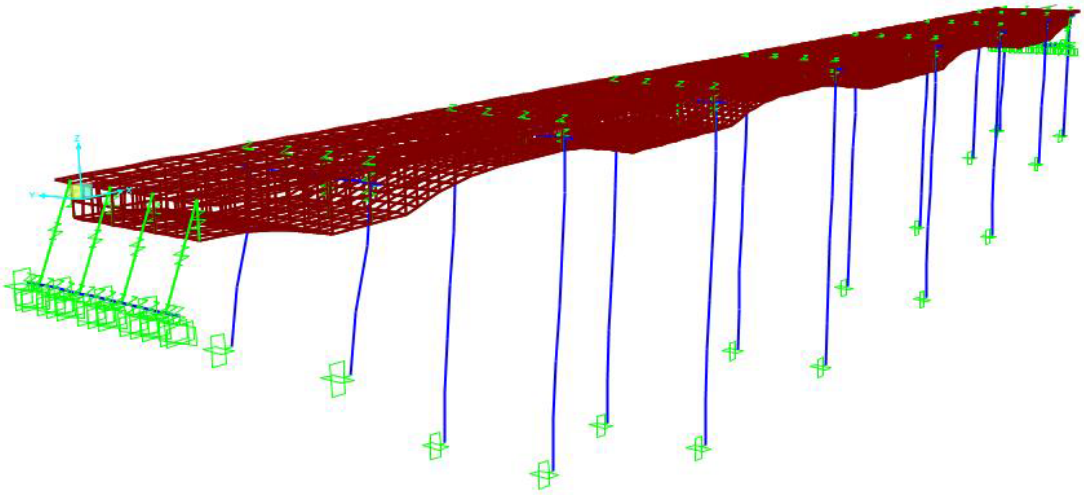

Figure 18: Deformed shape/ mode 5

3.2.2.7 Finite element model updating

The method applied minimizes in an iterative approach the differences between numerical and investigational modal parameters. The least square problem is resolved by the *Gauss-Newton* method. Practical execution of the Gauss-Newton method is based on the application of the singular value decomposition. The equation provided by Gauss-Newton is considered

similar to the truncated Taylor series applied in the penalty function process. The penalty function estimation is described by the following equation:

$$S\delta\theta - \delta z = 0$$

Where δz describes the difference between the measured modal data and the finite element result. Δθ illustrates the pertubation in the unidentified parameters to be updated. S is the sensitivity matrix that contains the first derivative of the estimated modal parameters- z with the respect to the unidentified ones- θ. A predetermined difference approximation is applied to estimate the elements of the sensitivity matrix. To decrease the number of update parameters a function is suggested that can portray a damage pattern by only a small amount representative parameters and that has the ability to cause snall as well as large damage zones. Presuming that the decrease of the bending stiffness can be assumed by the reduction of E modulus, the following result is proposed – more details are stated in Maeck (see reference). The stiffness rate reduses along the beam which corresponds with the outcome of the direct stiffness calculation. The fatigue function is applied in a non-symmetrical way.

Despite the fact that the mode shape information is only used in the case of direct stiffness calculation, it is as well implicitly applied in updating. Alterations of modal displacements are required to determined at which side the damage occurred on the structure that it is likely impossible by applying only eigen frequency information as the bridge model is considered point symmetrical.

This study represents an attempt to apply the functions of dynamic testing for the geometrically similar to ZB bridge project and a comparison between both experimental and calculated frequencies it is considered very encouraging at this early stage of the study. Furthermore, it is significant to note that the analysis appeared here is semi automatic. The variations in boundary conditions (i.e. the level of freedom for foundations to move) change the number of modes importantly and nonlinearly and hence the correlation and sensitivity analysis should be continued for every boundary condition. To prevail this limitation a complete three dimensional modal analysis is needed that has a clear number of modes for optimization even when it comes to relatively straightforward geometry of the footbridge.

3.2.2.8 Non linear effects

Even though the structure is considered to be relatively simple, the updating task is not trivial. Modal analysis is linear, however there are several of important non-linearities appeared in the model. The effects of the examination are listed as follows:

• The ground bend is non-linear, this is at the time, modeled with a single linear spring – a more composite method maybe required

• Throughout the tests it was clearly identified a very big amplitude dependant behavior of the modes. This is as well non-linear and hard to model.

• Non accessible site and data.

To investigate and resolve this situation, the dynamic response of the columns and foundations themselves require to be explored experimentally in greater detail. It is obvious indeed from the analysis that the movement of the foundations must be assessed in all axis directions. The number of movement is small and may be challenging to monitor them accurately. Innovative and more sophisticated optimization techniques will need to taken into consideration.

3.2.2.9 Dynamic testing – future damage detection

To achieve more accurate model predictions a more rich collection of information is required. This can be achieved by using sensors to track and collect accurate data regarding the existing model. There are for example sensors that can measure strain on the foundations on the base of the columns or for more accurate results the use of accelerometers to determine the dynamic stiffness rate of the foundations. Monitoring any alterations during damage accumulation will be vital for interpreting the data.

4 Modelling

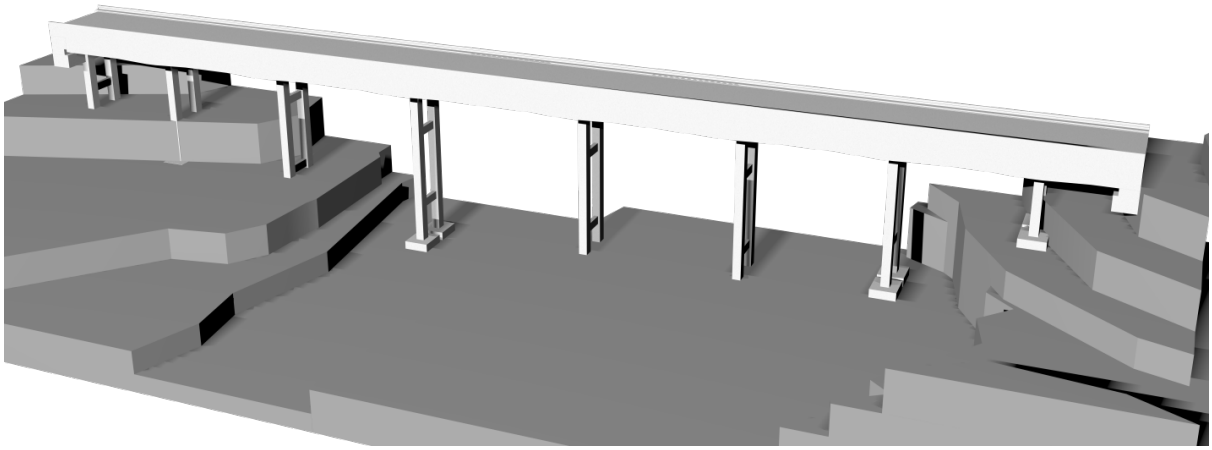

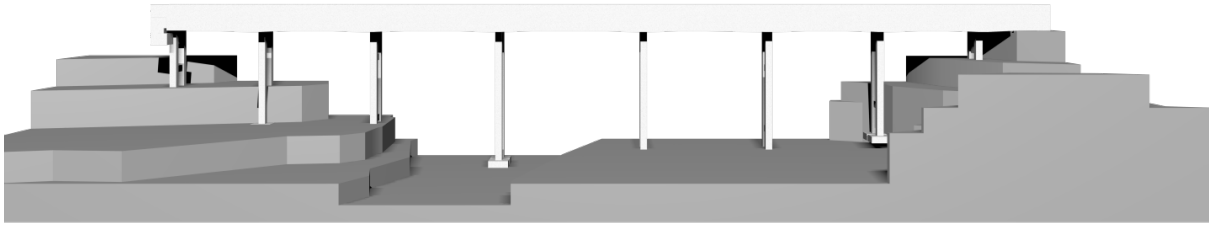

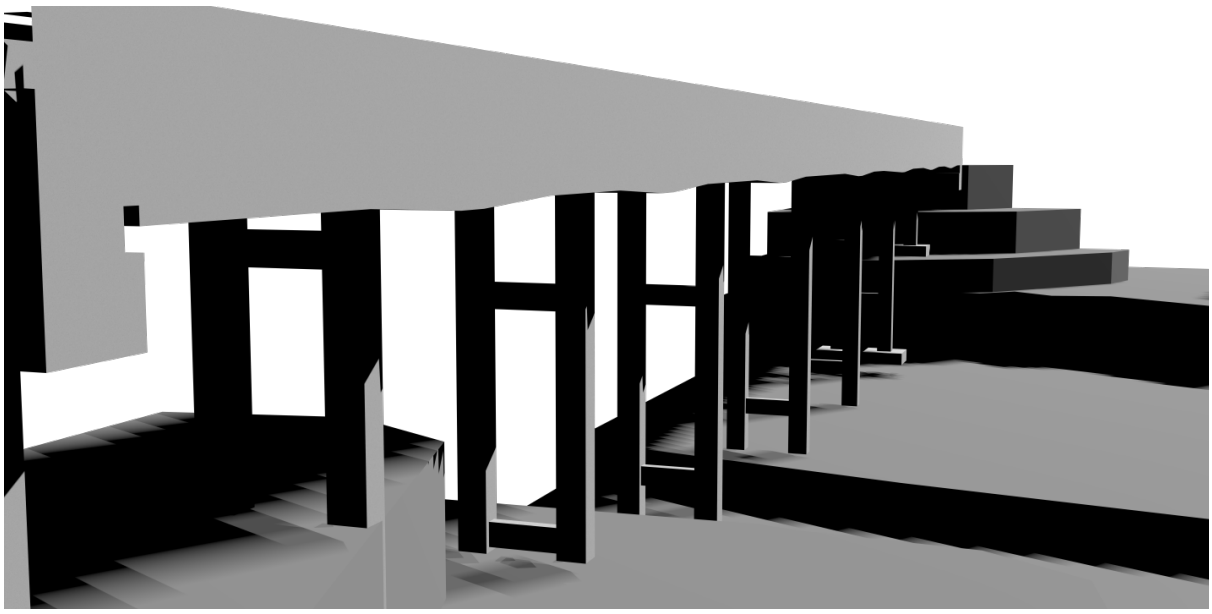

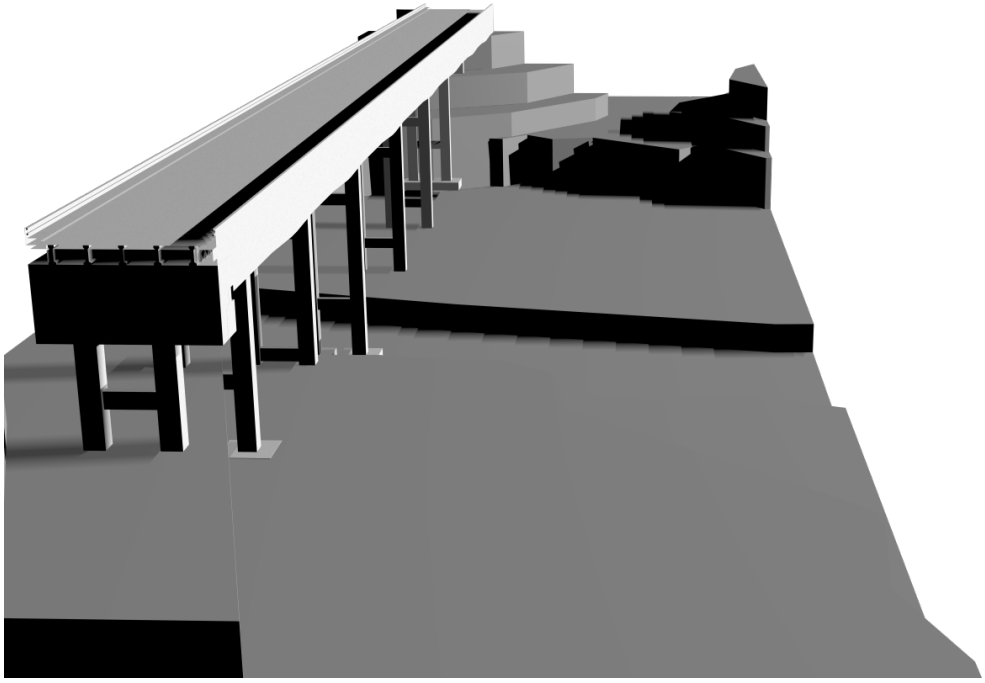

ΣΥΜΠΕΡΑΣΜΑΤΑ/ ΑΠΟΤΕΛΕΣΜΑΤΑ/ ΕΠΙΛΟΓΟΣ

An examination method is presented to embrace the result of cumulative seismic damage in columns in the Life cycle cost analysis of bridges. The examination method is comprehensive to account also for the structural damage due to the corrosion of the steel reinforcement. The unsureness in the ground motion parameters, seismic effect on the bridge, and corrosion process are accounted for in the examination method. The same methodology can also be applied to describe the uncertainties in the distance to the source and the mode of faulting. Through the use of an example bridge it is shown that the failure possibilities increase importantly over a bridge service-life. This is due to the damage accumulated while the repeated rate of small earthquakes that do not conduct to a failure of the bridge. It is also establish that, in seismic regions, the involvement of cumulative seismic damage is in higher rate than the one from corrosion. The expanded methodology can be applied in a LCC analysis to evaluate the optimal design parameters for a bridge. As a practical description, the suggested formulation is applied to evaluate the LCC of the example bridge and locate the optimal column diameter. The LCC analysis is also study the effect of various maintenance policies. It is established that although the bridge is deteriorating, preservation cost is considered higher than the expected failure cost due to the low probability of failure during its service life. Because of this reason, based on the LCC analysis, performing maintenance and inspections might not be economically necessary for bridges that are not considered as critical in the transportation network. The observations for the numerical example are exclusive to the example bridge for the selected seismic scenario case and environmental conditions. Nevertheless, the results are likely to be suitable also for other comparable bridges, scenarios, and conditions.

Direct stiffness calculation appears to be an excellent alternative to other observation methods such as sensitivity based updating techniques. Regardless of numerical inaccuracies at some locations of the bridge, the damage results were clearly observed and contained for the given settlements. For the considered bridge example higher modes appeared to offer bad results due to more numerical inaccuracies. In order to develop the method further, curvatures could be established experimentally, which is currently under investigation. Eigen frequencies as well as modal displacements are useful damage measures.

The outcomes of dynamic tests and modal analysis presented are considered a very useful tool for structural assessment, with the modal properties being responsive to a number of structural parameters. The model updating does not only progress our understanding of the total behavior of the example bridge, but also states the sensitivity to various parameters such as temperature, material parameters and boundary conditions. In developing the study further, it would help more accurate measurements of the example bridge, assessing sensor locations and calculation the variation of modal properties with value of the persuaded damage.

ΒΙΒΛΙΟΓΡΑΦΙΑ

1. Al-Harthy, A.S., Stewart, M.G., & Mullard, J. (2011). Concrete cover cracking caused by steel reinforcement corrosion. Magazine of Concrete Research, 63, 655–667.

2. Alonso, C., Andrade, J., Rodriguez, J., & Diez, J.M. (1998). Factors controlling cracking of concrete affected by reinforcement corrosion. Materials and Structures, 31, 435–441.

3. Apostolopoulos, C.A., & Papadakis, V.G. (2008). Consequences of steel corrosion on the ductility properties of reinforcement bar. Construction and Building Materials, 22, 2316–2324.

4. Bhargava K, Ghosh AK. Analytical model of corrosion-induced cracking of concrete considering the stiffness of reinforcement. Struct Eng Mech 2003;16:749–69.

5. Biondini, F., & Vergani, M. (2012). Damage modeling and nonlinear analysis of concrete bridges under corrosion. Sixth International Conference on Bridge Maintenance, Safety and Management (IABMAS 2012), Stresa, Italy, 8–12 July. In F. Biondini & D.M. Frangopol (Eds.), Bridge Maintenance, Safety, Management, Resilience and Sustainability. London: CRC Press/Balkema, Taylor & Francis Group.

6. Biondini, F., Bontempi, F., Frangopol, D.M., & Malerba, P.G. (2004a). Cellular automata approach to durability analysis of concrete structures in aggressive environments. ASCE Journal of Structural Engineering, 130, 1724–1737.

7. Campbell K. Empirical near-source attenuation relationship for horizontal and vertical components of peak ground acceleration, peak ground velocity, and pseudo-absolute acceleration response spectra. Seismological Research Letters 1997; 68(1):154–197.

8. Coronelli, D., & Gambarova, P. (2004). Structural assessment of corroded reinforced concrete beams: Modeling guidelines. ASCE Journal of Structural Engineering, 130, 1214–1224.

9. Coffin LF Jr. A study of the effects cyclic thermal stresses on a ductile metal. Transactions of the ASME 1954; 76:931–950.

10. Chernin L, Val DV, Volkh KY. Analytical modelling of concrete cover cracking caused by corrosion of reinforcement. Mater Struct 2010;43(4):543–56.

11. Chopra AK, Goel RK. Capacity-demand-diagram methods for estimating seismic deformation of inelastic structures: SDF systems. Report Number PEER-1999/02, Pacific Earthquake Engineering Research Center, University of California, Berkeley, CA, 1999.

12. Das S, Gupta VK, Srimahavishnu V. Damage based design with no repairs for multiple events and its sensitivity to seismicity model. Earthquake Engineering and Structural Dynamics 2006; 36(3):307–325.

13. Du, Y.G., Clark, L.A., & Chan, A.H.C. (2005). Residual capacity of corroded reinforcing bars. Magazine of Concrete Research, 57, 135–147.

14. Dura-Crete. Statistical quantification of the variables in the limit state functions. Report No. BE95-1347/R7, The European Union Brite EuRam 3 contract BRPR-CT95-0132 Project BE95-1347, 2000.

15. Enright, M.P.(1998) “Time-variant reliability of reinforced concrete bridges under environmental attack”. *The Philosophy Doctor Thesis of University of Colorado*. Denver：University of Colorado.

13. Friswell M I and Mottershead J E 1995 Finite Element Model Updating in Structural Dynamics (Dordrecht: Kluwer)

16. IMSL Library Reference Manual. International Mathematical and Statistical Libraries (IMSL), Houston, Texas (1984).

17. Kong JS, Frangopol DM. Life-cycle reliability-based maintenance cost optimization of deteriorating structureswith emphasis on bridges. Journal of Structural Engineering 2003; 129(6):818–828.

18. Kunnath SK, El-Bahy A, Taylor AW, Stone WC. Cumulative seismic damage of reinforced concrete bridge piers.NISTIR 6075, National Institute of Standards and Technology, Gaithersburg, MD, U.S.A., 1997.

19. Kunnath SK, Chai YH. Cumulative damage-based inelastic demand spectrum. Earthquake Engineering and Structural Dynamics 2004; 33(4):499–520.

20. Liu Y, Weyers R. Modeling the time-to-corrosion cracking in chloride contaminated reinforced concrete structures. ACI Mater J 1998;95(6):675–81.

21. Maeck J, Abdel Wahab M and De Roeck G 1998 Damage detection in reinforced concrete structures by dynamic system identification Proc. ISMA 23, Noise and Vibration Engineering (Leuven, Belgium, 1998) pp 939–46

22. Mander JB, Panthaki FD, Kasalanati A. Low-cycle fatigue behavior of reinforcing steel. Journal of Materials in Civil Engineering 1994; 6(4):453–468.

23. Manson SS. Behavior of materials under conditions of thermal stress. Heat Transfer Symposium, University of Michigan Engineering Research Institute, 1953; 9–75.

24. Miner MA. Cumulative damage in fatigue. Journal of Applied Mechanics (ASME) 1945; 12:A159–A164.

25. Mori, Y., Ellingwood, B.R. (1993a) “Time-dependen System Reliability Analysis” *Adaptive Importance Sampling.Sturctural Safety* ,15(1)：59-73

26. Peeters, B., and De Roeck, G. _2001_. “Stochastic system identification for operational modal analysis: A review.” *J. Dyn. Syst., Meas., Control*, 123_4_, 659–667.

27. Torres-Acosta, A.A., & Martinez-Madrid, M. (2003). Residual life of corroding reinforced concrete structures in marine environment. ASCE Journal of Materials in Civil Engineering, 15, 344–353.

28. Tsuno K, Park R. Prediction method for seismic damage reinforced concrete bridge columns. Journal of StructuralMechanical Earthquake Engineering 2004; 21(2):97–111.

29. Val, D.V., & Melchers, R.E. (1997). Reliability of deteriorating RC slab bridges. ASCE Journal of Structural Engineering, 123, 1638–1644.

30. Vidal, T., Castel, A., & Francois, R. (2004). Analyzing crack width to predict corrosion in reinforced concrete. Cement and Concrete Research, 34, 165–174.

31. Vu, K., Stewart, M.G., & Mullard, J. (2005). Corrosion-induced cracking: experimental data and predictive models. ACI Structural Journal, 102, 719–726

32. Wen YK, Kang YJ. Minimum building life-cycle cost design criteria. I: methodology. Journal of Structural Engineering 2001; 127(3):330–337.